Inhibition of the mevalonate pathway improves myocardial fibrosis

HUIFENG XU[1], YI SHEN[2], CHENYU LIANG[1], HAIFENG WANG[2],
JUNLING HUANG[2], PENGCHENG XUE[1] and MING LUO[1]

Departments of [1]Cardiology and [2]Geriatrics, Tongji Hospital Affiliated to Tongji University, Shanghai 200065, P.R. China

Abstract. The mevalonate (MVA) pathway serves an important role in ventricular remodeling. Targeting the MVA pathway has protective effects against myocardial fibrosis. The present study aimed to investigate the mechanism behind these effects. Primary cultured cardiac fibroblasts from C57BL/6 mice were treated *in vitro* in 5 groups: i) negative control; ii) angiotensin II (Ang II) model ($1x10^{-5}$ mol/l); iii) Ang II + rosuvastatin (ROS); iv) Ang II + alendronate (ALE); and v) Ang II + fasudil (FAS). Collagen and crystal violet staining were used to assess morphological changes in cardiac fibroblasts. Reverse transcription quantitative PCR and western blotting were used to analyze the expression of key signaling molecules involved in the MVA pathway. Collagen staining in the ALE, FAS, and ROS groups was weak compared with the Ang II group, while the rate of cell proliferation in the ROS, ALE, and FAS groups was slower compared with that in the Ang II group. In addition, the expression of key signaling molecules in the MVA pathway, including transforming growth factor-β1 (*TGF-β1*), heat shock protein 47 (*HSP47*), collagen type I α1 (*COL1A1*), vascular endothelial growth factor 2 (*VEGF2*) and fibroblast growth factor 2 (*FGF2*), was decreased in the FAS and ROS groups compared with the Ang II model. Compared with the Ang II group, 3-Hydroxy-3-Methylglutaryl-CoA reductase (*HMGCR*) gene expression was significantly lowered in the drug intervention groups, whereas farnesyl pyrophosphate synthase (*FDPS*) expression was downregulated in the ALE group, but elevated in the FAS and ROS groups. Compared with that in the Ang II group, ras homolog family member A (*RhoA*) expression was downregulated in the FAS and ROS groups, whilst mevalonate kinase expression was reduced in the ROS group. Protein expression of TGF-β1, COL1A1 and HSP47 were decreased following intervention with each of the three drugs compared

with the Ang II group. Overall, rosuvastatin, aledronate and fasudil decreased the proliferation of myocardial fibroblasts and inhibited collagen synthesis. Rosuvastatin had the strongest protective effects against myocardial fibrosis compared with the other drugs tested, suggesting this to be a potential agent for the clinical treatment of cardiovascular disease.

Introduction

The mevalonate (MVA) pathway is indispensable for *de novo* synthesis of cholesterol as well as other molecules essential for various cellular functions, including cell proliferation and apoptosis (1). MVA is irreversibly synthesized from 3-hydroxy-3-methylglutaryl-coenzyme A (HMG-CoA), and further metabolized into farnesyl diphosphate, which is also called farnesyl pyrophosphate (FPP), and geranylgeranyl pyrophosphate (2). These isoprenoids are precursors for a number of important metabolites, including sterols, dolichols, ubiquinones (also known as coenzyme Q) and carotenoids (3).

HMG-CoA reductase (HMGCR) is the rate-limiting enzyme in cholesterol biosynthesis, which catalyzes the conversion of HMG-CoA to MVA (1). Statin drugs are capable of inhibiting the synthesis of endogenous cholesterol by competitive inhibition of HMGCR (4). Statins were originally used to treat hypercholesterolemia (5), but have since been found to exert many pleiotropic effects (6), including immunomodulatory, anti-inflammatory (7), and neuroprotective (8) effects. Clinical studies have demonstrated that statins can be used to treat diseases that are not clearly related to low-density lipoprotein cholesterol (LDL-C) or cholesterol (9,10). This may be due to the inhibitory effect of statins on the production of isoprenoid intermediates in the cholesterol biosynthesis pathway (9,11). Post-translational prenylation of small guanosine triphosphate binding proteins, such as Rho and Rac, and their downstream effectors, such as Rho kinase and nicotinamide adenine dinucleotide phosphate oxidase, is also inhibited by statins (6). However, the use of statins in the treatment of heart failure remains controversial (12-14).

In a previous study, it was demonstrated that rats given a high-salt diet developed high blood pressure, diastolic heart dysfunction and increased rates of myocardial fibrosis (15). Transcriptome analysis demonstrated that the MVA pathway served an important role in the pathophysiology of myocardial fibrosis (15,16). Other studies have also indicated the relevance of

Correspondence to: Dr Ming Luo, Department of Cardiology, Tongji Hospital Affiliated to Tongji University, 389 Xincun Road, Shanghai 200065, P.R. China
E-mail: lmfc84@126.com

key enzymes and downstream GTPases, including Rho and Ras, in the MVA pathway to myocardial fibrosis (17,18). Inhibition of Rho and Ras can reduce myocardial hypertrophy and fibrosis (17). The present study used multiple drugs, including rosuvastatin, alendronate, and fasudil, which regulate the MVA pathway at different points. Rosuvastatin, one of the most commonly used drugs in secondary prevention of cardiovascular disease, is a potent, effective, and safe HMGCR inhibitor (19,20). Alendronate is a farnesyl pyrophosphate synthase (FDPS) inhibitor that improved vascular endothelial function in a hypertensive rat model (21,22). Fasudil is a clinically used Rho/Rho associated coiled-coil containing protein kinase (ROCK) inhibitor that has a good therapeutic effect in cardiovascular diseases including angina, hypertension, and coronary spasms (23,24). By observing the effects of these drugs on myocardial fibroblasts, the present study explored the mechanism by which the MVA pathway is involved in myocardial fibrosis. The present study could provide new directions and theoretical basis for the development of novel targeted drugs, as well as for the clinical treatment and prevention of diastolic heart failure and myocardial fibrosis.

Materials and methods

Isolation and primary culture of cardiac fibroblasts. A total of 10 C57BL/6 male mice (6 weeks; weight, 20±2 g) were obtained from the Shanghai Experimental Animal Center of the Chinese Academy of Sciences and kept in a climate-controlled room (temperature, 25±1˚C; relative humidity, 50-60%; free access to food and water; and 12-h light/dark cycle.) for 1 week of acclimatization. All experimental protocols involving live animals were reviewed and approved by the Institutional Animal Care and Use Committee of the Tongji Hospital of Tongji University (approval no. 2019-DW-008) (Shanghai, China). Murine cardiac fibroblasts were isolated as previously described (25,26). In short, C57BL/6 mice were anaesthetized with 3% isoflurane until loss of limb reflexes.

Hearts were isolated from C57 mice at room temperature (RT) and subjected to 5 min perfusion with DMEM/F12 supplemented with 1% penicillin, 1% streptomycin, and 1% amphotericin B solution (all Gibco; Thermo Fisher Scientific, Inc.) at RT. The hearts were perfused with collagenase type II (Gibco; Thermo Fisher Scientific, Inc.) at 37˚C for 20 min before dissociation of the tissue at RT and incubation with dilute collagenase (0.05% w/v) at 37˚C for 10 min. The collagenase was neutralized by adding 2X the existing volume of DMEM/F12 complete medium supplemented with 10% FBS (Gibco; Thermo Fisher Scientific, Inc.). The cell suspension was then passed through a 40-μm sterile cell strainer to remove undigested tissue. The filtered suspension was collected and centrifuged at 500 x g for 10 min at room temperature. After centrifugation, the supernatant was discarded and the cell pellet was resuspended in 10 ml growth medium (DMEM/F12 with 10% FBS) and then diluted to a final volume of 30 ml. Cells were seeded in cell culture dishes and allowed to adhere for 2 h in 5% CO_2 at 37˚C. The cell cultures were moved into T-25 flasks (4 ml cell suspension) and incubated overnight at 37˚C. The following day, the cultures were washed twice with phosphate-buffered saline (PBS) and the growth medium was replaced. The culture medium was replaced once per day in this way until harvesting after 3 days.

Flow cytometry. Third-generation cardiac fibroblasts were prepared into a single cell suspension with 0.25% trypsin and the cell density was adjusted to $1x10^6$ cells/ml. The cells were fixed and permeabilized with FIX & PERM Cell Permeabilization Kit (cat. no. GAS003; Thermo Fisher Scientific, Inc.) at 37˚C for 30 min. The cells were then incubated at 37˚C for 30 min with PBS and anti-vimentin antibody (1:100, cat. no. ab92547; Abcam), before being incubated with FITC-labeled secondary antibody (1:1000, cat. no. ab6717) at 37˚C for 30 min. Cells were then analyzed using a BD FACSCanto™ II flow cytometer (BD Biosciences) with FlowJo software (Version 7.6, BD Biosciences).

Drug intervention experiment and cell staining. A total of five treatment groups were established for the fibroblasts: i) negative control (NC); ii) angiotensin II (Ang II) model, iii) Ang II + rosuvastatin (ROS); iv) Ang II + alendronate (ALE), and v) Ang II + fasudil (FAS). The drug concentrations were based on preliminary experiments: Ang II, $1x10^{-5}$ mol/l; rosuvastatin, $1x10^{-5}$ mol/l; alendronate, $1x10^{-6}$ mol/l and fasudil, 10 μg/ml. The fibroblasts were treated with the drugs for 48 h at 37˚C. No drugs were added to the NC group. For crystal violet staining, the medium was discarded and the cells were fixed with 10% methanol for 30 sec at RT, followed by staining with 0.5% crystal violet staining solution for 20 min at RT. Cell morphology was observed by light microscopy (magnification, x100).

For collagen staining, the medium was discarded following drug intervention and the cells were fixed with 4% paraformaldehyde for 30 min at RT, and stained using Masson's Trichrome Stain Kit according to the manufacturer's instructions (cat. no. G1340, Beijing Solarbio Science & Technology Co., Ltd.). Cell collagen staining was observed by light microscopy (magnification, x100).

Cell proliferation assay. Cell proliferation was assessed using the Cell Counting Kit-8 (CCK-8) (Dojindo Molecular Technologies Inc.). Briefly, cells were seeded in 96-well plates at $1x10^4$ cells/well and treated with drugs for 0, 24 and 48 h. CCK-8 solution (5 μl) was added to each well and incubated at 37˚C for an additional 2 h. Optical density (OD) was determined at 450 nm.

Reverse transcription-quantitative (RT-q) PCR. Total RNA of cells was extracted with TRIzol® (Invitrogen; Thermo Fisher Scientific Inc.). cDNA synthesis was carried out using a TOYOBO ReverTra Ace qPCR RT kit (Toyobo Life Science) and qPCR was performed using the SYBR Supermix PCR kit (Kapa Biosystems; Roche Diagnostics), according to the manufacturer's protocols. Primers were obtained from Sangon Biotech Co., Ltd. and the sequences are listed in Table I. The reverse transcription reaction step as follows: 37˚C for 15 min and 95˚C for 5 min. The thermocycling conditions were as follows: Initial denaturation at 95˚C for 5 min, followed by 40 cycles of 95˚C for 30 sec, 61˚C for 30 sec and 72˚C for 30 sec. Gene expression levels were measured using cycle threshold (CQ) values and the $2^{-\Delta\Delta Cq}$ calculation (27) and normalized to GAPDH.

Western blotting. RIPA buffer (cat. no. 9806; Cell Signaling Technologies Inc.) was used for cells protein extraction and protein concentration was determined using bicinchoninic acid protein assay reagent (cat. no. 7780; Cell Signaling

Table I. Primer sequences used for reverse transcription-quantitative polymerase chain reaction.

Gene name	Primer sequence (5' to 3')	Amplicon size (bp)
GAPDH	F: GCAAGTTCAACGGCACAGTCA	
	R: ACGACATACTCAGCACCAGCAT	127
HMGCR	F: CTTGACGCTCTGGTGGAATG	
	R: GTTGGCAAGCACGGACATAC	105
FDPS	F: AGCAGAATTTCATCCAGCACT	
	R: GTCAGACCCCGATTGTACT	148
RhoA	F: ATGTGGCAGATATTGAAGTGGA	
	R: GTGTCTGGGTAGGAGAGAGG	106
FGF-2	F: ACCCACACGTCAAACTACAG	
	R: GGCGTTCAAAGAAGAAACACTC	150
TGF-β1	F: CCTGAGTGGCTGTCTTTTGA	
	R: CGTGGAGTACATTATCTTTGCTG	124
VEGF	F: ACTGGACCCTGGCTTTACT	
	R: ATTGGACGGCAATAGCTGC	136
COL1A1	F: GACGCATGGCCAAGAAGAC	
	R: ACTTCTGCGTCTGGTGATAC	234
HSP47	F: GTCCATCAACGAGTGGGC	
	R: CAGTGCGGCTTAAAGAACATG	117
MVD	F: GTCAACATCGCGGTTATCAA	
	R: CCTCTGTGAAGTCCTTGCTAA	142
MVK	F: CCAAACGTCGGTATTAAGCA	
	R: GCCTTCGTTGCCTACACA	159

HSP47, heat shock protein 47; COL1A1, collagen type I α1; HMGCR, HMG-CoA reductase; FDPS, farnesyl pyrophosphate synthase; MVD, mevalonate diphosphate decarboxylase; MVK, mevalonate kinase; FGF-2, fibroblast growth factor-2; VEGF, vascular endothelial growth factor.

Technologies Inc.). A total of 50-100 μg protein/lane were subjected to SDS-PAGE (10% gel) and transferred onto a PVDF membrane. The membrane was blocked by 5% non-fat milk powder for 1 h at room temperature before incubation with the following primary antibodies: TGF-β1 (1:1,000; cat. no. ab92486; Abcam), collagen I (1:1,000; cat. no. ab34710; Abcam), heat shock protein 47 (HSP47; 1:1,000; cat. no. ab109117; Abcam) or GAPDH (1:4,000; cat. no. E12-042; EnoGene Biotech Co., Ltd.) at 4˚C overnight. Goat-anti-rabbit antibody (1:2,000; cat. no. ab205718; Abcam) was used as the secondary antibody at RT for 1 h. Chemiluminescent visualization was performed using ECL reagent (cat. no. 32106; Pierce; Thermo Fisher Scientific Inc.). The protein loading control was GAPDH. Optical density analysis was performed by ImageJ software (version 1.8, National Institutes of Health).

Statistical analysis. GraphPad Prism v.7.0 (Graph Pad Inc.) was used for statistical analysis. The data is expressed as the means ± SD from experimental repeats. The comparison of multiple groups was performed using one-way analysis of variance followed by the post hoc Tukey's test. $P<0.05$ was considered to indicate a statistically significant difference.

Results

Fibroblast cell identification. We performed primary cultures of cardiac fibroblasts and identified by flow staining. Microscopically, the fibroblast cell bodies were large and spindle-shaped or stellate and flat with multiple spindles (Fig. 1A). DAPI staining shows regular oval nuclei (Fig. 1B). Anti-vimentin FITC was detected on the surface of 98.7% of cultured cells (Fig. 1C and D).

Drug therapy alleviate the process of Ang II-promoted cell fibrosis. Cells were large and mostly spindle-shaped in the NC group (Fig. 2A). Cells were proliferative and growth was dense and radial in the Ang II group (Fig. 2A). There was no significant difference in cell morphology between the ALE and Ang II groups (Fig. 2A). The FAS and ROS groups had fewer cells, more cytoplasm, and some cells were round compared with those in the Ang II group (Fig. 2A). Collagen fiber staining in the Ang II group was significantly more intense compared with that in the NC group (Fig. 2A). Collagen staining in the ALE, FAS, and ROS groups was weak compared with the Ang II group (Fig. 2A). These results suggested that drug intervention can significantly inhibit the Ang II-induced increase in collagen level in myocardial cells. Ang II can significantly promote proliferation compared with that in the NC group, whilst the rates of proliferation in the ROS, ALE and FAS treatment groups were lower compared with those in the Ang II group at both 24 and 48 h (Fig. 2B). This indicated that drug therapy can alleviate the process of Ang II-promoted cell fibrosis.

mRNA expression levels of MVA pathway and fibrosis-related genes under different drug interventions. Subsequently,
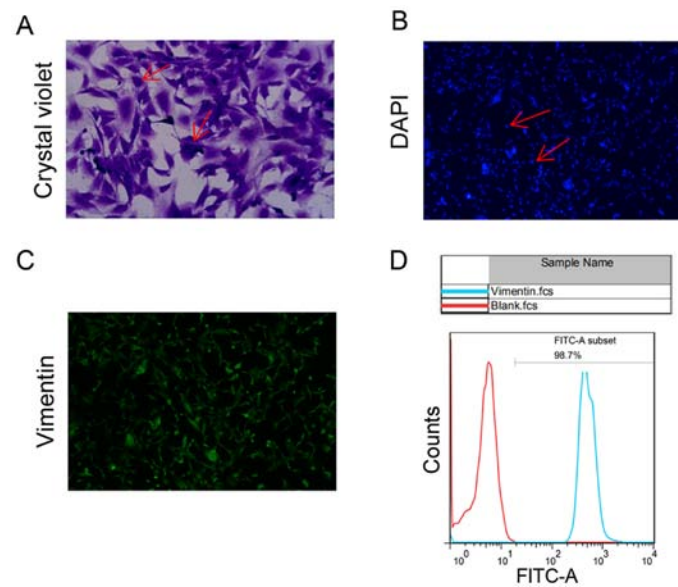
Figure 1. Primary cultures and identification of cardiac fibroblasts. (A) Crystal violet staining shows cell bodies were large and spindle-shaped or stellate and flat with multiple spindles (as shown by the arrows). Magnification, x200. (B) DAPI staining shows regular cell nuclei (as shown by the arrows). Magnification, x100. (C) Anti-vimentin-FITC was detected, (D) where vimentin was detected on the surface of 98.7% of the cultured cells by flow cytometry. Magnification, x100.
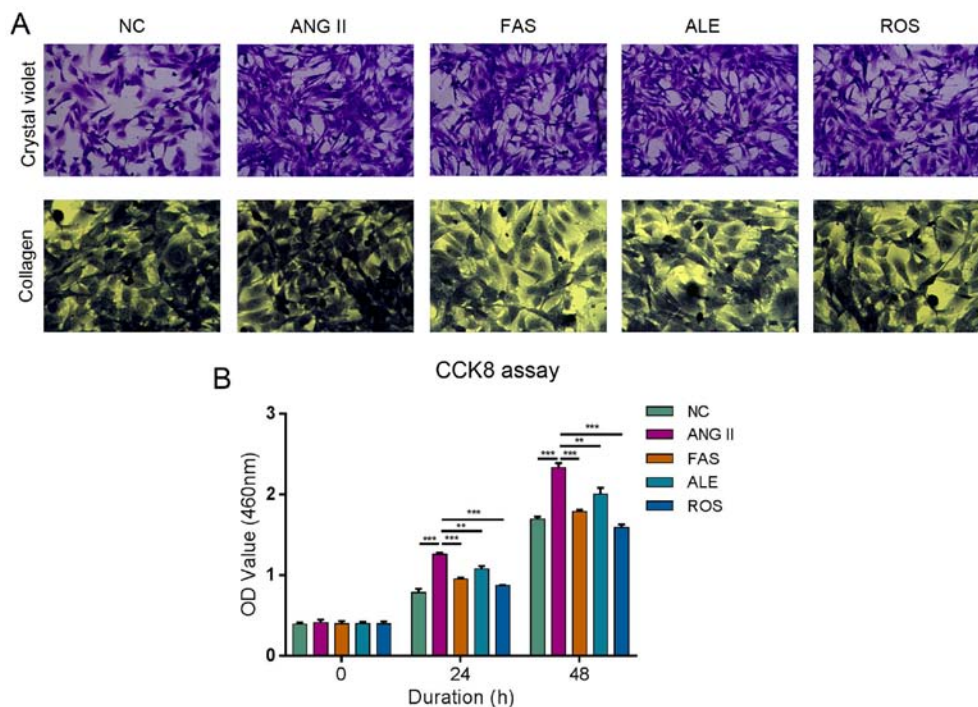

Figure 2. ALE, FAS and ROS therapy alleviate the process of Ang II-promoted cell fibrosis and viability of cardiac fibroblasts. (A) Crystal violet staining (magnification, x200) shows cells were proliferative and growth was dense in the Ang II group. There was no difference in cell morphology between the ALE and Ang II groups. The FAS and ROS groups had fewer cells, more cytoplasm, and some cells were round compared with those in Ang II group. Collagen staining (magnification, x200) in the Ang II group was more intense compared with that in the NC group. ALE, FAS, and ROS groups was weak compared with the Ang II group. (B) Cell proliferation assay shows Ang II significantly promote proliferation compared with NC group, whilst the rates of proliferation in the ROS, ALE, and FAS treatment groups were lower compared Ang II group at both 24 and 48 h. $^{**}P<0.01$ and $^{***}P<0.001$. NC, negative control; Ang II, angiotensin II; ROS, Ang II + rosuvastatin; ALE, Ang II + alendronate; FAS, Ang II + fasudil.

effects of rosuvastatin, fasudil and alendronate on gene expression in cultured primary cardiac fibroblasts were investigated by RT-qPCR. After 72 h treatment with the different drug interventions, relative mRNA abundance of genes including *TGF-β1*, *HSP47*, collagen type I α1 (*COL1A1*), *HMGCR*, *FDPS*, ras homolog family member A (*RhoA*), mevalonate diphosphate decarboxylase (*MVD*), mevalonate kinase (*MVK*), fibroblast growth factor-2 (*FGF-2*), and vascular endothelial growth factor (*VEGF*) was examined. *TGF-β1, HSP47, COL1A1, VEGF* and *FGF2* expression was

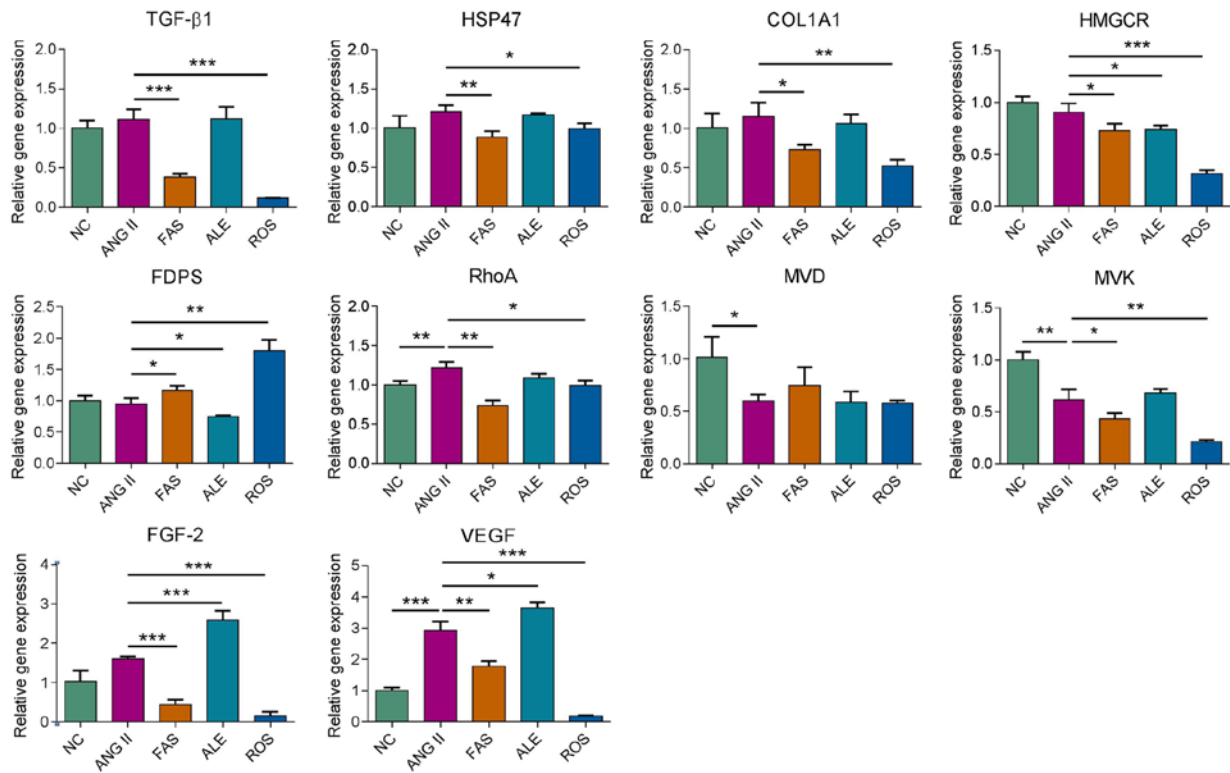Figure 3. Reverse transcription-quantitative polymerase chain reaction analysis of the genetic regulatory effects of drug treatment. $^*P<0.05$, $^{**}P<0.01$, $^{***}P<0.001$. NC, negative control; ROS, Ang II + rosuvastatin; ALE, Ang II + alendronate; FAS, Ang II + fasudil; HSP47, heat shock protein 47; COL1A1, collagen type I α1; HMGCR, HMG-CoA reductase; FDPS, farnesyl pyrophosphate synthase; MVD, mevalonate diphosphate decarboxylase; MVK, mevalonate kinase; Ang II, angiotensin II; FGF-2, fibroblast growth factor-2; VEGF, vascular endothelial growth factor.
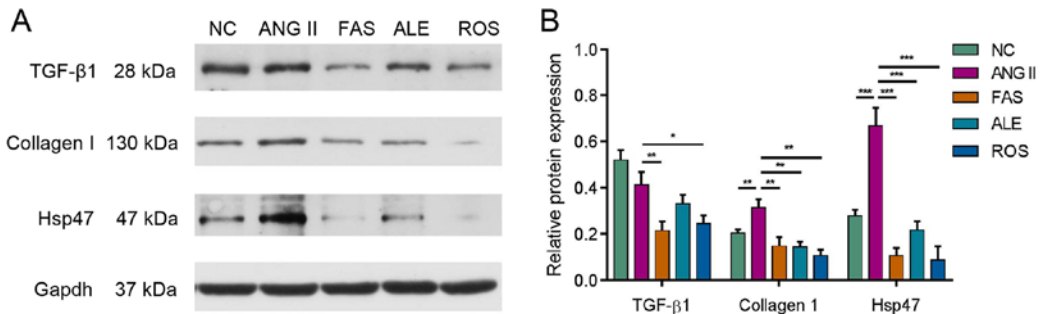

Figure 4. Fibrosis-related protein expression after drug treatment. Western blotting assay (A) and densitometric analysis (B) of the effects of drug treatment on protein expression in cultured myocardial fibroblasts. Data are presented relative to GAPDH. Protein expression of TGF-β1, collagen I and HSP47 were decreased following drug treatment compared with the Ang II group. ($^*P<0.05$, $^{**}P<0.01$ and $^{***}P<0.001$). NC, negative control; Ang II, angiotensin II; HSP47, heat shock protein 47; ROS, Ang II + rosuvastatin; ALE, Ang II + alendronate; FAS, Ang II + fasudil.

significantly reduced in the FAS and ROS groups compared with the Ang II group (Fig. 3). *HMGCR* expression was significantly lower in the drug intervention groups compared with that in the Ang II group. *FDPS* expression was downregulated in the ALE group and elevated in the FAS and ROS groups compared with the Ang II group (Fig. 3). *RhoA* expression was downregulated in the FAS and ROS groups compared with the Ang II group and the expression of *MVK* was decreased in the ROS group compared with the other groups (Fig. 3). The results indicated rosuvastatin, fasudil and alendronate can target different target genes that regulate the MVA pathway and interfere with the expression of fibrosis-related genes.

Fibrosis-related protein expression. Western blotting was used to analyze expression of key signaling molecules involved in myocardial fibrosis, including TGF-β1, collagen I and HSP47. Ang II stimulation resulted in a significant increase in collagen I and HSP47 expression (Fig. 4). Protein expression of TGF-β1, collagen I and HSP47 all decreased following drug treatment compared with the Ang II group (Fig. 4).

Discussion

Statins have been used for several decades to prevent hypercholesterolemia and cardiovascular diseases, including hyperlipidemia and atherosclerosis (19,20). The primary

mechanism of action of statin drugs is the lowering of serum cholesterol (28). However, statins may exert cardiovascular protective effects that are independent of LDL-C lowering, such as pleiotropic effects (29). The mechanism of these effects may be related to suppression of the MVA pathway and downstream GTPase activity (30,31).

Some cell culture and animal studies have suggested that statins can prevent the development of cardiac hypertrophy and fibrosis (32-35), which may reduce ventricular compliance and is a major cause of cardiac diastolic dysfunction (36). A meta-analysis of 11 eligible studies, including 17,985 patients with heart failure with a preserved ejection fraction demonstrated that statin therapy may be associated with improved survival rates in these patients (37). However, 2 large-scale randomized controlled studies of patients with chronic heart failure (the CORONA and GISSI-HF trials) demonstrated that the majority of patients exhibited heart failure with a reduced ejection fraction. The aforementioned studies demonstrated that compared with the control groups, the use of statins did not reduce the primary outcome (death from any cause) (12,14).

The present study demonstrated that rosuvastatin can inhibit the increased collagen levels in myocardial fibroblasts caused by Ang II, reduce the proliferation of myocardial fibroblasts induced by Ang II, and significantly decrease the gene expression of *FGF-2*, *TGF-β1*, *VEGF* and *COL1A1*, and the protein expression of TGF-β1, collagen I, and HSP47. HSP47 is a collagen-specific molecular chaperone residing in the endoplasmic reticulum (38). HSP47 is essential for collagen synthesis in vertebrates (39). Previous studies have shown that inhibition of HSP47 can improve the phenotype of collagen-related diseases, such as pulmonary artery fibrosis, peritoneal fibrosis, and liver fibrosis (40-42). In addition, HSP47 has been found to be associated with fibrosis level after myocardial infarction (43). Another study suggested that the beneficial effect of atorvastatin on cardiac fibrosis may be due to lowered HSP47 levels (34). The results of the present study are consistent with the aforementioned studies, with statins having the strongest effect among the tested drugs. The results of the present study suggested that statins have antimyocardial fibrosis effects and may have clinical therapeutic potency for the treatment of diastolic heart failure.

FDPS is a key enzyme in the MVA pathway (44). This chain-elongation enzyme catalyzes head-to-tail condensation of 2 molecules of isopentenyl diphosphate with dimethylallyl diphosphate to form FPP (45). FPP is an important intermediate in cholesterol and sterol biosynthesis, a substrate for protein farnesylation and geranylgeranylation and a ligand for certain hormone receptors and growth receptors, such as thyroid hormone nuclear receptor-β (TR-β) and farnesoid X receptor (46). Prenylation of small GTP-binding proteins by FPP is critical for enabling such proteins to be incorporated into membranes, hence determining their localization and function, and serving a crucial role in signal transduction (47). Previous studies have demonstrated that compared with Wistar Kyoto rats, the expression of FDPS is significantly increased in aortic smooth muscle cells and in the left ventricles of spontaneously hypertensive rats (SHR) (48). Upregulation of FDPS has also been detected in the heart and abdominal aorta in rat models of overload-induced cardiac hypertrophy and associated diastolic dysfunction (49). Additionally, cardiac-specific overexpression of FDPS has been demonstrated to induce cardiac hypertrophy, fibrosis, and heart failure (18). These pathological changes were associated with the activation of RhoA and other known kinases, including ERK1/2 and p38 MAPK in the hypertrophic signaling pathway (18). FDPS inhibitors, namely nitrogen-containing bisphosphonate (N-BP), are commonly used to treat osteoporosis and osteolytic bone lesions (50). Previous studies have demonstrated that N-BP may have effects on the cardiovascular system (21,22,51). Ibandronate, a potent N-BP has been demonstrated to reduce reactive oxygen species production in the vascular smooth muscle of SHR rats (21), improve vascular endothelial function (21) and prevent noradrenaline-induced fibrosis of vascular smooth muscle (22). Another previous study also suggested that chronic treatment with alendronate can reduce myocardial hypertrophy and fibrosis whilst improving aortic remodeling through a pathway involving inhibition of the geranylgeranylation and activation of RhoA (52).

The present study demonstrated that alendronate reversed the proliferation of myocardial fibroblasts induced by Ang II. Collagen staining suggested that aledronate can inhibit the increase of collagen levels of myocardial fibroblasts induced by Ang II. However, alendronate had the weakest effect among the three chosen drugs in the present study. In addition, alendronate did not decrease the mRNA expression of *TGF-β1*, *COL1A1*, *VEGF* or *FGF-2* in the present study, which suggested that alendronate has limited preventative effects in myocardial fibrosis and collagen synthesis. This result is inconsistent with those of previous studies (21,22,53). This may be because the doses of N-BP were much larger in the animal models used (50-100 times the doses used in humans) (53). The effect in these previous studies was positively associated with the duration of drug administration (21,22,53). The present study was an *in vitro* one in which the optimal concentration and duration of alendronate treatment remain to be identified. There are 2 types of signaling pathways involved in Ang II activation: G protein-dependent and -independent pathways. Alendronate only affects the G protein-dependent pathway allowing Ang II to continue to promote fibrosis via other pathways, including the epidermal growth factor receptor and insulin receptor signaling pathways (21,22).

The small GTPase, RhoA, belongs to the Rho GTPase family, part of the Ras-like GTP-binding protein superfamily, whose members serve important roles in the regulation of cytoskeletal dynamics, cell adhesion and migration (54). RhoA controls actin stress fiber formation and acto-myosin contraction at the rear of the cell (54). The RhoA/ROCK signaling pathway is closely associated with a number of cardiovascular and cerebrovascular diseases, including coronary atherosclerotic heart disease, stroke, and pulmonary vascular disease (55-57). Evidence has suggested that RhoA is intricately involved in the pathophysiology of cardiac diseases (58). Constitutive overexpression of RhoA in cardiomyocytes leads to the spontaneous development of dilated cardiomyopathy, heart failure, and bradycardia (59). RhoA/ROCK activation is required for the development of fibrosis in animal models of cardiac fibrosis as well as fibrosis of other organs, such as the lung, liver, and kidney (60). Fasudil is a clinically applied Rho-kinase-inhibitor, which has demonstrated therapeutic effects against cerebral vasospasm after subarachnoid hemorrhage (61). Fasudil has also been demonstrated to have various

biological roles in the cardiovascular system and cardioprotective functions in myocardial ischemia/reperfusion (I/R) injury animal models. These examples include improvements in coronary vasodilation, inhibition of apoptosis and oxidative stress, relieving inflammation and reduction in endoplasmic reticulum stress and metabolism (24). However, the mechanism of fasudil action remains unclear. In the present study, fasudil increased collagen levels of myocardial fibroblasts induced by Ang II, prevented their proliferation, significantly reduced the mRNA expression of *FGF-2, TGF-β1, VEGF, COL1A1*, and *HSP47*, and the protein expression of TGF-β1, HSP47, and collagen I. The efficacy of fasudil was similar to that of rosuvastatin and slightly lower compared with that of the statin. Considering that statins act on HMGCR, the rate-limiting enzyme of the MVA pathway (4), while fasudil acts on downstream small GTPases (23), it is speculated that the antimyocardial fibrosis effect induced by inhibition of the MVA pathway is largely due to the inhibition of small GTPases.

The findings of the present study suggested that 3 drugs acting at different points in the MVA pathway (rosuvastatin, aledronate, and fasudil) can all inhibit the proliferation and collagen synthesis of myocardial fibroblasts induced by Ang II, with the strongest effect induced by rosuvastatin and the weakest by aledronate. Results from the present study could provide new directions and theoretical basis for the clinical treatment and prevention of diastolic heart failure and the regulation of myocardial fibrosis.

Acknowledgements

Not applicable.

Funding

Availability of data and materials

The datasets used and/or analyzed during the current study are available from the corresponding author on reasonable request

Authors' contributions

HX and ML designed the present study. HX, YS, CL, HW and JH performed the experiments. HX, ML and PX analyzed the data. HX and ML are responsible for confirming this authenticity of all the raw data. All authors read and approved the final manuscript.

Ethics approval and consent to participate

All experimental protocols involving live animals were reviewed and approved by the Institutional Animal Care and Use Committee of the Tongji Hospital of Tongji University (approval no. 2019-DW-008; Shanghai, China).

Patient consent for publication

Not applicable.

Competing interests

The authors declare that they have no competing interests.

References

1. Goldstein JL and Brown MS: Regulation of the mevalonate pathway. Nature 343: 425-430, 1990.
2. Bathaie SZ, Ashrafi M, Azizian M and Tamanoi F: Mevalonate Pathway and Human Cancers. Curr Mol Pharmacol 10: 77-85, 2017.
3. Yeganeh B, Wiechec E, Ande SR, Sharma P, Moghadam AR, Post M, Freed DH, Hashemi M, Shojaei S, Zeki AA, et al: Targeting the mevalonate cascade as a new therapeutic approach in heart disease, cancer and pulmonary disease. Pharmacol Ther 143: 87-110, 2014.
4. Ference BA, Ray KK, Catapano AL, Ference TB, Burgess S, Neff DR, Oliver-Williams C, Wood AM, Butterworth AS, Di Angelantonio E, et al: Mendelian Randomization Study of ACLY and Cardiovascular Disease. N Engl J Med 380: 1033-1042, 2019.
5. Raper A, Kolansky DM and Cuchel M: Treatment of familial hypercholesterolemia: Is there a need beyond statin therapy? Curr Atheroscler Rep 14: 11-16, 2012.
6. Oesterle A, Laufs U and Liao JK: Pleiotropic effects of statins on the cardiovascular system. Circ Res 120: 229-243, 2017.
7. Steffens S and Mach F: Anti-inflammatory properties of statins. Semin Vasc Med 4: 417-422, 2004.
8. Greenwood J, Steinman L and Zamvil SS: Statin therapy and autoimmune disease: From protein prenylation to immunomodulation. Nat Rev Immunol 6: 358-370, 2006.
9. Ward NC, Watts GF and Eckel RH: Statin toxicity. Circ Res 124: 328-350, 2019.
10. Schleyer T, Hui S, Wang J, Zhang Z, Knapp K, Baker J, Chase M, Boggs R and Simpson RJ Jr: Quantifying unmet need in statin-treated hyperlipidemia patients and the potential benefit of further LDL-C reduction through an EHR-based retrospective cohort study. J Manag Care Spec Pharm 25: 544-554, 2019.
11. Toth PP and Banach M: Statins: Then and now. Methodist Debakey Cardiovasc J 15: 23-31, 2019.
12. Nochioka K, Sakata Y, Miyata S, Miura M, Takada T, Tadaki S, Ushigome R, Yamauchi T, Takahashi J and Shimokawa H; CHART-2 Investigators: Prognostic impact of statin use in patients with heart failure and preserved ejection fraction. Circ J 79: 574-582, 2015.
13. Kjekshus J, Apetrei E, Barrios V, Böhm M, Cleland JG, Cornel JH, Dunselman P, Fonseca C, Goudev A, Grande P, et al; CORONA Group: Rosuvastatin in older patients with systolic heart failure. N Engl J Med 357: 2248-2261, 2007.
14. Liu G, Zheng XX, Xu YL, Ru J, Hui RT and Huang XH: Meta-analysis of the effect of statins on mortality in patients with preserved ejection fraction. Am J Cardiol 113: 1198-1204, 2014.
15. Xu H, Qing T, Shen Y, Huang J, Liu Y, Li J, Zhen T, Xing K, Zhu S and Luo M: RNA-seq analyses the effect of high-salt diet in hypertension. Gene 677: 245-250, 2018.
16. Li X, Han J, Li L, Wang KJ and Hu SJ: Effect of farnesyl-transferase inhibition on cardiac remodeling in spontaneously hypertensive rats. Int J Cardiol 168: 3340-3347, 2013.
17. Zhao CZ, Zhao XM, Yang J, Mou Y, Chen B, Wu HD, Dai DP, Ding J and Hu SJ: Inhibition of farnesyl pyrophosphate synthase improves pressure overload induced chronic cardiac remodeling. Sci Rep 6: 39186, 2016.
18. Yang J, Mou Y, Wu T, Ye Y, Jiang JC, Zhao CZ, Zhu HH, Du CQ, Zhou L and Hu SJ: Cardiac-specific overexpression of farnesyl pyrophosphate synthase induces cardiac hypertrophy and dysfunction in mice. Cardiovasc Res 97: 490-499, 2013.
19. Perez-Calahorra S, Laclaustra M, Marco-Benedi V, Pinto X, Sanchez-Hernandez RM, Plana N, Ortega E, Fuentes F and Civeira F: Comparative efficacy between atorvastatin and rosuvastatin in the prevention of cardiovascular disease recurrence. Lipids Health Dis 18: 216, 2019.
20. Wander GS, Hukkeri MYK, Yalagudri S, Mahajan B and Panda AT: Rosuvastatin: Role in Secondary Prevention of Cardiovascular Disease. J Assoc Physicians India 66: 70-74, 2018.
21. Han J, Jiang DM, Ye Y, Du CQ, Yang J and Hu SJ: Farnesyl pyrophosphate synthase inhibitor, ibandronate, improves endothelial function in spontaneously hypertensive rats. Mol Med Rep 13: 3787-3796, 2016.

22. Du CQ, Yang L, Yang J, Han J, Hu XS, Wu T and Hu SJ: Inhibition of farnesyl pyrophosphate synthase prevents norepinephrine-induced fibrotic responses in vascular smooth muscle cells from spontaneously hypertensive rats. Hypertens Res 37: 26-34, 2014.

23. Oh KS, Oh BK, Park CH, Seo HW, Kang NS, Lee JH, Lee JS and Ho Lee B: Cardiovascular effects of a novel selective Rho kinase inhibitor, 2-(1H-indazole-5-yl)amino-4-methoxy-6-piperazino triazine (DW1865). Eur J Pharmacol 702: 218-226, 2013.

24. Huang YY, Wu JM, Su T, Zhang SY and Lin XJ: Fasudil, a Rho-kinase inhibitor, exerts cardioprotective function in animal models of myocardial ischemia/reperfusion injury: a meta-analysis and review of preclinical evidence and possible mechanisms. Front Pharmacol 9: 1083, 2018.

25. Landry NM, Rattan SG and Dixon IMC: An improved method of maintaining primary murine cardiac fibroblasts in two-dimensional cell culture. Sci Rep 9: 12889, 2019.

26. Ackers-Johnson M, Li PY, Holmes AP, O'Brien SM, Pavlovic D and Foo RS: A simplified, Langendorff-free method for concomitant isolation of viable cardiac myocytes and nonmyocytes from the adult mouse heart. Circ Res 119: 909-920, 2016.

27. Livak KJ and Schmittgen TD: Analysis of relative gene expression data using real-time quantitative PCR and the 2(-Delta Delta C(T)) µethod. Methods 25: 402-408, 2001.

28. Alonso R, Cuevas A and Cafferata A: Diagnosis and management of statin intolerance. J Atheroscler Thromb 26: 207-215, 2019.

29. Krähenbühl S, Pavik-Mezzour I and von Eckardstein A: Unmet veeds in LDL-C lowering: when statins won't do! Drugs 76: 1175-1190, 2016.

30. Sethunath V, Hu H, De Angelis C, Veeraraghavan J, Qin L, Wang N, Simon LM, Wang T, Fu X, Nardone A, *et al*: Targeting the mevalonate pathway to overcome acquired anti-HER2 treatment resistance in breast cancer. Mol Cancer Res 17: 2318-2330, 2019.

31. Longo J, Mullen PJ, Yu R, van Leeuwen JE, Masoomian M, Woon DTS, Wang Y, Chen EX, Hamilton RJ, Sweet JM, *et al*: An actionable sterol-regulated feedback loop modulates statin sensitivity in prostate cancer. Mol Metab 25: 119-130, 2019.

32. Wu CK, Yeh CF, Chiang JY, Lin TT, Wu YF, Chiang CK, Kao TW, Hung KY and Huang JW: Effects of atorvastatin treatment on left ventricular diastolic function in peritoneal dialysis patients-The ALEVENT clinical trial. J Clin Lipidol 11: 657-666, 2017.

33. Beck AL, Otto ME, D'Avila LB, Netto FM, Armendaris MK and Sposito AC: Diastolic function parameters are improved by the addition of simvastatin to enalapril-based treatment in hypertensive individuals. Atherosclerosis 222: 444-448, 2012.

34. Akahori H, Tsujino T, Naito Y, Matsumoto M, Sasaki N, Iwasaku T, Eguchi A, Sawada H, Hirotani S and Masuyama T: Atorvastatin ameliorates cardiac fibrosis and improves left ventricular diastolic function in hypertensive diastolic heart failure model rats. J Hypertens 32: 1534-1541, discussion 1541, 2014.

35. Choi SY, Park JS, Roh MS, Kim CR, Kim MH and Serebruany V: Inhibition of angiotensin II-induced cardiac fibrosis by atorvastatin in adiponectin knockout mice. Lipids 52: 415-422, 2017. Erratum in: Lipids 52: 1061, 2017.

36. Vasan RS, Benjamin EJ and Levy D: Congestive heart failure with normal left ventricular systolic function. Clinical approaches to the diagnosis and treatment of diastolic heart failure. Arch Intern Med 156: 146-157, 1996.

37. Fukuta H, Goto T, Wakami K and Ohte N: The effect of statins on mortality in heart failure with preserved ejection fraction: A meta-analysis of propensity score analyses. Int J Cardiol 214: 301-306, 2016.

38. Florkowski CM, Molyneux SL and George PM: Rosuvastatin in older patients with systolic heart failure. N Engl J Med 358: 1301, author reply 1301, 2008.

39. Ito S and Nagata K: Roles of the endoplasmic reticulum-resident, collagen-specific molecular chaperone Hsp47 in vertebrate cells and human disease. J Biol Chem 294: 2133-2141, 2019.

40. Brown KE, Broadhurst KA, Mathahs MM, Brunt EM and Schmidt WN: Expression of HSP47, a collagen-specific chaperone, in normal and diseased human liver. Lab Invest 85: 789-797, 2005.

41. Nishino T, Miyazaki M, Abe K, Furusu A, Mishima Y, Harada T, Ozono Y, Koji T and Kohno S: Antisense oligonucleotides against collagen-binding stress protein HSP47 suppress peritoneal fibrosis in rats. Kidney Int 64: 887-896, 2003.

42. Hagiwara S, Iwasaka H, Matsumoto S and Noguchi T: Introduction of antisense oligonucleotides to heat shock protein 47 prevents pulmonary fibrosis in lipopolysaccharide-induced pneumopathy of the rat. Eur J Pharmacol 564: 174-180, 2007. Retraction in: Eur J Pharmacol 792: 80, 2016.

43. Sauk JJ, Nikitakis N and Siavash H: Hsp47 a novel collagen binding serpin chaperone, autoantigen and therapeutic target. Front Biosci 10: 107-118, 2005.

44. Sun S and McKenna CE: Farnesyl pyrophosphate synthase modulators: A patent review (2006-2010). Expert Opin Ther Pat 21: 1433-1451, 2011.

45. Dhar MK, Koul A and Kaul S: Farnesyl pyrophosphate synthase: A key enzyme in isoprenoid biosynthetic pathway and potential molecular target for drug development. N Biotechnol 30: 114-123, 2013.

46. Vukelic S, Stojadinovic O, Pastar I, Vouthounis C, Krzyzanowska A, Das S, Samuels HH and Tomic-Canic M: Farnesyl pyrophosphate inhibits epithelialization and wound healing through the glucocorticoid receptor. J Biol Chem 285: 1980-1988, 2010.

47. Hooff GP, Wood WG, Müller WE and Eckert GP: Isoprenoids, small GTPases and Alzheimer's disease. Biochim Biophys Acta 1801: 896-905, 2010.

48. Chen GP, Yao L, Lu X, Li L and Hu SJ: Tissue-specific effects of atorvastatin on 3-hydroxy-3-methylglutarylcoenzyme A reductase expression and activity in spontaneously hypertensive rats. Acta Pharmacol Sin 29: 1181-1186, 2008.

49. Chen B, Zhong LY, Yang JX, Pan YY, Chen F, Yang J, Wu T and Hu SJ: Alteration of mevalonate pathway related enzyme expressions in pressure overload-induced cardiac hypertrophy and associated heart failure with preserved ejection fraction. Cell Physiol Biochem 32: 1761-1775, 2013.

50. Holstein SA: A patent review of bisphosphonates in treating bone disease. Expert Opin Ther Pat 29: 315-325, 2019.

51. Sing CW, Wong AY, Kiel DP, Cheung EY, Lam JK, Cheung TT, Chan EW, Kung AW, Wong IC and Cheung CL: Association of alendronate and risk of cardiovascular events in patients with hip fracture. J Bone Miner Res 33: 1422-1434, 2018.

52. Yang J, Chen YN, Xu ZX, Mou Y and Zheng LR: Alteration of RhoA prenylation ameliorates cardiac and vascular remodeling in spontaneously hypertensive rats. Cell Physiol Biochem 39: 229-241, 2016.

53. Susic D, Varagic J, Ahn J, Slama M and Frohlich ED: Beneficial pleiotropic vascular effects of rosuvastatin in two hypertensive models. J Am Coll Cardiol 42: 1091-1097, 2003.

54. Schaefer A, Reinhard NR and Hordijk PL: Toward understanding RhoGTPase specificity: Structure, function and local activation. Small GTPases 5: 6, 2014.

55. Vesterinen HM, Currie GL, Carter S, Mee S, Watzlawick R, Egan KJ, Macleod MR and Sena ES: Systematic review and stratified meta-analysis of the efficacy of RhoA and Rho kinase inhibitors in animal models of ischaemic stroke. Syst Rev 2: 33, 2013.

56. Sun Z, Wu X, Li W, Peng H, Shen X, Ma L, Liu H and Li H: RhoA/rock signaling mediates peroxynitrite-induced functional impairment of Rat coronary vessels. BMC Cardiovasc Disord 16: 193, 2016.

57. Antoniu SA: Targeting RhoA/ROCK pathway in pulmonary arterial hypertension. Expert Opin Ther Targets 16: 355-363, 2012.

58. Loirand G, Sauzeau V and Pacaud P: Small G proteins in the cardiovascular system: Physiological and pathological aspects. Physiol Rev 93: 1659-1720, 2013.

59. Sah VP, Minamisawa S, Tam SP, Wu TH, Dorn GW II, Ross J Jr, Chien KR and Brown JH: Cardiac-specific overexpression of RhoA results in sinus and atrioventricular nodal dysfunction and contractile failure. J Clin Invest 103: 1627-1634, 1999.

60. Shimizu T and Liao JK: Rho kinases and cardiac remodeling. Circ J 80: 1491-1498, 2016.

61. Hasegawa S, Hasegawa Y and Miura M: Current therapeutic drugs against cerebral vasospasm after subarachnoid hemorrhage: a comprehensive review of basic and clinical studies. Curr Drug Deliv 14: 843-852, 2017.